Am J Cancer Res 2022;12(5):2160-2172
www.ajcr.us /ISSN:2156-6976/ajcr0141043

Original Article

Long noncoding RNA UCA1 promotes carboplatin resistance in retinoblastoma cells by acting as a ceRNA of miR-206

Nanye Wang[1], Huimin Fan[1], Shuhua Fu[1], Shaojun Li[1], Bin Zhou[2], Qifang Jin[1], Zhipeng You[1]

[1]Department of Ophthalmology, The Second Affiliated Hospital of Nanchang University, Nanchang 330006, Jiangxi, China; [2]Department of Orthopedics, The Second Affiliated Hospital of Nanchang University, Nanchang 330006, Jiangxi, China

Received December 9, 2021; Accepted April 19, 2022; Epub May 15, 2022; Published May 30, 2022

Abstract: Chemoresistance has become a major obstacle to effective retinoblastoma treatment. The urothelial cancer-associated gene 1 (*UCA1*) is commonly considered an oncogene in certain types of cancer and is related to drug resistance. Nonetheless, the molecular mechanism and effect of *UCA1* in carboplatin resistance in retinoblastoma are unclear. In this study, *UCA1* expression was determined by sequential screening and lncRNA profile analysis, which is highly abundant in carboplatin-resistant retinoblastoma cells. Functional analyses revealed that *UCA1* promoted carboplatin resistance by promoting c-Met and AXL expression. Mechanistic studies revealed that *UCA1* facilitated c-Met and AXL expression as a ceRNA of miR-206. Importantly, retinoblastoma nude mouse model experiments revealed that targeting *UCA1* or c-Met and AXL can restore drug sensitivity in carboplatin-resistant retinoblastoma. Collectively, we found that *UCA1* is a mediator of carboplatin resistance in retinoblastoma cells. It competes with others as the endogenous RNA of miR-206, thus upregulating its targets, c-MET and AXL expression.

Keywords: Retinoblastoma, carboplatin resistance, UCA1, miR-206, AXL/c-Met

Introduction

Retinoblastoma (RB) is a primary intraocular malignant tumour occurring most frequently in children [1]. Recently, with the development of surgical procedures such as enucleation and various chemotherapy methods, the survival rate of patients with retinoblastoma has improved [2]. However, the mortality rate associated with RB remains high because of its limited sensitivity to chemotherapy [3, 4]. Therefore, understanding the molecular events of chemoresistance in retinoblastoma and formulating molecular targeted treatment strategies are essential for the treatment of this malignant disease.

Long-chain non-coding RNAs (lncRNAs) are a group of non-coding RNA subsets with no obvious protein-coding function, and their lengths exceed 200 nucleotides [5, 6]. LncRNAs are involved in multilevel gene expression regulation, including transcriptional regulation by recruiting complexes modified by chromatin, and post-transcriptional adjustment by interacting with proteins, mRNAs, or miRNA [7-9]. New evidence indicates that lncRNAs regulate many characteristics of cancer, including chemoresistance, apoptosis, and proliferation [10-13].

The urothelial cancer-associated gene 1 (*UCA1*), which is located on chromosome 19p13.12, was first discovered in bladder cancer. It facilitates the progression of cancer in various tumours through the regulation of proliferation, migration, apoptosis, and invasion of cells [14-16]. More importantly, in addition to its carcinogenic function, *UCA1* also regulates drug resistance in various types of cancer. For instance, *UCA1* facilitates cell proliferation and leads to 5-fluorouracil resistance in patients with colon cancer [17]. A reduced expression of *UCA1* can increase chemosensitivity and apoptosis in tongue squamous cell carcinoma cells induced by Cisplatin (CDDP) [18, 19]. However, the role of *UCA1* in carboplatin resistance remains

unclear. In the present study, we investigated the effect of *UCA1* on carboplatin resistance and simultaneously explored the therapeutic importance of carboplatin resistance in patients with the condition.

Methods

Cell lines and reagents

From the American Type Culture Collection (ATCC, Rockville, MD, USA), we acquired the cell lines of human retinoblastoma WERI-Rb1 (HTB-169) and Y79 (HTB-18), which were cultivated in McCoy's 5a (Life Technologies) or RPMI-1640 (Gibco) together with heat-inactivated fetal bovine serum (10%, Gibco; Thermo Fisher Scientific, Inc.), under a temperature of 37°C, 10% of ultimate concentration was reached in the humidified incubator involving 5% CO_2.

In vivo xenograft and treatment experiments

Male non-thymic BALB/C nude mice aged between 4 and 6 weeks were fed with the standard sterile environments. The animal study was authorized through the Animal Experiment Ethics Committee of the Second Affiliated Hospital of Nanchang University. The xenograft volume was assessed with two vertical diameter calipers, calculated as below: V = [length/^{2}] × [width^2]. Xenograft specimens were collected for transplantation or rapidly frozen in liquid nitrogen until ready for use. To obtain carboplatin resistant retinoblastoma cells, the nude mice flank was subcutaneously injected with 5 × 10^6 Y79 or WERI-Rb1 cells. When xenograft volume up to 200 mm^3, carrier or carboplatin (CBP, 40 mg/kg/day) were injected intraperitoneally for 4 weeks and 2 weeks according to the standard treatment scheme. After a course of treatment, the xenograft retinoblastoma cells were isolated and transplanted into nude mice again, and then treated with carrier or carboplatin. retinoblastoma cells were isolated from the third generation xenotransplantation and confirmed to be carboplatin resistant retinoblastoma cells (called YCR3rd and WCR3rd). In order to isolate xenograft tumor cells, the xenograft was mechanically decomposed with 500 μg/mL of streptomycin and 500 U/mL of penicillin, 2.5 mg/L of amphotericin B and 100 mg/L of gentamicin were cleaned with cold PBS, digested in RPMI-1640 medium involving 1 mg/ml DNase and 1 mg/ml type II or IV collagenase under a temperature of 37°C for 60 minutes, and also shaken intermittently. The cell suspension was passed through 80 μm filter (BD Biosciences, USA) and centrifuge at 300 g at 4°C for 5 minutes. The precipitates were suspended and inoculated in 6-well plates. Mice xenografted with YCR3rd cells were intraperitoneally injected with carboplatin (40 mg/kg/day). When the size of xenografts was matched, mice were randomly assigned to intravenous injection of in vivo grade LNA (50 nmol, twice a week), intraperitoneal injection of carboplatin (40 mg/kg/day), or combined treatment for 4 weeks. Exiqon (Denmark) designed and synthesized in vivo grade LNA targeting UCA1 (5'-gtctgccatatag-3') or disturbing LNA (5'-aacacgttctacgc-3'). In addition, mice xenografted with ycr3rd cells were intraperitoneally injected with carboplatin (40 mg/kg/day), bms-777607 (10 mg/kg/day) or combined treatment for 12 weeks. Bms777607 (10 mg/kg/day), or combination therapy for 12 weeks.

RNA isolation and qRT-PCR assay

In accordance with the guidelines of manufacturer, TRIzol reagent (Invitrogen) was exploited for extracting and gathering the overall RNA from cells or tissues. From the above total RNA (1 μg), the first strand cDNA was generated via applying miScript reverse transcription kit (Qiagen, Dusseldorf, Germany). miScript SYBR-Green PCR kit (Qiagen) was subsequently employed for quantifying miR-206 and UCA1 expression levels. qRT-PCR primers are as follows: *UCA1* forward: 5'-TTTATGCTTGAGCCTTGA-3', reverse 5'-CTTGCCTGAAATACTTGC-3'; c-Met forward: 5'-TGAGAAGGCTAAAGGAAACG-3', reverse 5'-TGGACCGTCAAGAAGTAAAT-3'; AXL forward: 5'-GACCCGTTATGGAGAAGTGT-3', reverse 5'-GGAGTCGTCCTGGTTGAGC-3'. $2^{-\Delta\Delta CT}$ strategy was exploited for calculating the relative fold change of the gene expression, where U6 snRNA or GAPDH was used as an internal control.

shRNAs and plasmids

Short hairpin RNA *UCA1* (sh*UCA1*) or shNC was transferred into cells by the lentivirus, labeled as the sh*UCA1* group and shNC group, respectively. After successful transfection, the cells were collected for Western blot, qRT-PCR and CCK8. Detailed target sequences of shRNA

were as follows: sh-*UCA1-1*: 5'-CTCCTGGAAGCCACAAGATTA-3' and sh-*UCA1-2* 5'-GTTAATCCAGGAGACAAAGA-3' (Gene Pharmaceutical Co., Ltd., Shanghai, China). *UCA1* cDNA was amplified using PrimeSTAR HS DNA polymerase (Takara, China) and subcloned into the pcDNA3.1 vector, which is known as pcDNA3.1-UCA1. pcDNA3.1-UCA1 containing a miR-206 MRE point mutation was constructed by GenePharma Co., Ltd. and named pcDNA3.1-UCA1 (mut). Based on the specifications of the manufacturer, Lipofectamine RNAiMAX (Invitrogen, USA) was conducted to transfect siRNA and plasmids (China Gene Pharmaceutical) or miR-206 mimic or inhibitor (China Ribobio).

The human AXL and c-MET open reading frame (ORF) sequences were amplified from the ORF cloning vector purchased from GenePharma Co., Ltd., and subcloned into the pLenti III vector. shRNA oligonucleotides were synthesised by GenePharma Co., Ltd. After annealing, the double-stranded oligomer was inserted into the lentivirus pLKO. 1-Puro vector (Addgene). The lentiviral vector and packaging vector were co-transfected into HEK-293T cells to prepare lentiviruses.

Colony formation and cell proliferation assays

Cell Counting Kit 8 (Dojindo, Japan) was used to measure RB cell viability, at OD 450 nm, which was subsequently detected using the BioTek Gen5 system (BioTeck, USA). In the colony generation experiment, RB cells (1000 cells/well) were inoculated into a 6-well plate. After cultivation in a humidified chamber at 5% CO_2 at 37°C for two weeks, the cells were cleaned with PBS, stained with 0.1% crystal violet for 15 min, and finally cleaned twice using PBS.

Cell apoptosis detection

The carboplatin (10 μM) was used to treat carboplatin-resistant (CR) RB cells at various transfection rates for two days, which were subsequently double-stained using the Annexin V FITC/PI Apoptosis Detection Kit (BD Biosciences) according to the manufacturer's instructions. Flow cytometry (BD Biosciences, USA) was employed for assessing the rate of apoptosis.

Western blotting

The overall cell protein was extracted from lysed cells and granulosa cells, and RIPA buffer (China Aidlab Biotechnology, Inc.) was added with a protease inhibitor (Roche). After separating SDS-PAGE and transferring the membrane, the cells were seeded with the following primary antibodies: anti-p-EGFR (1:1000, CST), anti-EGFR (1:1000, Abcam), anti-pc-MET (1:1000, Abcam), anti-c-MET (1:1000, Abcam), anti-p-AXL (1:1000, CST), anti-AXL (1:1000, Abcam), and anti-GADPH (1:1000, Abcam), followed by treatment with 1:1000 HRP-conjugated secondary antibody. Finally, the protein bands were observed using a chemiluminescence detection kit (Aidlab Biotechnology, Inc., China), which was then quantified using Image Lab 4.0 software (Bio-Rad).

RNA immunoprecipitation (RIP) assays

In accordance with the manufacturer's instructions, the Magna RIP RNA binding protein immunoprecipitation kit (Millipore, USA) was used for RIP experiments. Ago2 (1:50; Merck Millipore) was used to detect RIP. When RIP is treated with RNase, the lysate and RNase are cultivated for 60 min at 37°C. RT-PCR detection of the co-precipitated RNA was performed.

Luciferase reporter assay

The lncRNA UCA1 containing wild type and mutant type was amplified, and then, inserted into the Luciferase reporter vector psiCHECK-2 (Promega, Madison, WI, USA) to construct the vector of WT-UCA1 and MUT-UCA1. Then, the WT-UCA1 or MUT-UCA1 was co-transfected with miR-206 or NC into the YCR3rd or WCR3rd cells using Lipofectamine 2000 reagent (Invitrogen, Carlsbad, MA, USA). After two days of transfection, the dual-luciferase reporter gene analysis system (Promega, Madison, WI, USA) was used to detect luciferase activity.

Statistical analyses

The data are described with the mean ± SD of three separated researches. The one-way analysis of variance and Student's t test were employed for analyzing the difference between multiple groups and between two groups, respectively, and then use Dunnett's post-hoc test to analyze. SPSS 19.0 (IBM) was implemented for all of the statistical calculations, and all the charts were established with GraphPad Prism 8.0 (GraphPad software). P less than 0.05 was regarded as statistically significant difference.

Results

UCA1 is highly expressed in CR RB cells

To acquire CR RB cells, WERI-RB-1 and Y79 cells were transplanted into nude mice, and carboplatin treatment cycles were implemented together with continuous passages *in vivo* (**Figure 1A**). The xenografts of RB from the third generation showed adverse reactions to carboplatin treatment (**Figure 1B**). From these xenografts, the drug-resistant RB cells were separated and referred to as WCR3rd and YCR3rd. In contrast to parental cells, WCR3rd and YCR3rd cells showed a lower response to carboplatin. After treatment with carboplatin, DIC50 increased, apoptosis was reduced, and growth ability was enhanced (**Figure 1C** and **1D**).

To determine the lncRNA needed for carboplatin resistance of RB, microarray was used to compare the expression profiles of lncRNAs between CR and parental RB cells. The heat map shows a significant difference between the parental and resistant cells (**Figure 1E**). The six lncRNAs with the largest difference (fold change > 5) were verified via qRT-PCR. Finally, we focused on the lncRNA *UCA1* with the greatest change (**Figure 1F**).

UCA1 is required for carboplatin resistance of RB

To investigate the functional effect of *UCA1* on carboplatin resistance, we knocked down *UCA1* statically in CR cells via short hairpin RNA (shRNA) mediated by the lentivirus (**Figure 2A**). The obvious decrease in IC50 and growth suppression after treatment with carboplatin was caused by the silencing of *UCA1* in drug-resistant cells (**Figure 2B** and **2C**). In addition, when exposed to carboplatin, the downregulation of *UCA1* resulted in increased apoptosis of WCR3rd and YCR3rd cells compared to the Sh-NC group (**Figure 2D** and **2E**). Also, *UCA1* knockdown significantly restored the sensitivity of the YCR3rd xenograft to carboplatin *in vivo* (**Figure 2F**). In summary, these data indicate that *UCA1* is the principal regulator of carboplatin resistance in RB cells.

AXL and c-Met are responsible for UCA1-mediated carboplatin resistance in RB

We deeply explored the mediators of *UCA1* that drive carboplatin resistance. There is increasing evidence that alternative Receptor Tyrosine Kinase (RTK) activation exerts a significant effect on drug resistance [20]. As a result, in drug-resistant cells, multiple RTKs were screened and it was discovered that the knockdown of *UCA1* decreased the phosphorylation levels of c-Met and AXL and the expression of protein and mRNA (**Figure 3A** and **3B**). Nevertheless, other RTKs, such as EGFR, do not possess *UCA1* differences after changing the above genes. High c-Met and AXL expression were observed in the CR xenografts (**Figure 3C**).

Next, we investigated whether c-Met and AXL participate in carboplatin resistance mediated by *UCA1*. The recovery of c-Met and AXL replicated the CR phenotype in *UCA1* resistant cells (**Figure 3D**, **3E** and Supplementary Figure 1). On the contrary, the simultaneous downregulation of c-Met and AXL can eliminate the effect of *UCA1*-mediated carboplatin resistance on cell viability, and the impact of reducing only the two is limited (**Figure 3F** and Supplementary Figure 2). In addition, BMS777607, which is a small molecule suppression of c-Met and AXL [21], re-sensitising *UCA1* excessively expressed cells to carboplatin (**Figure 3G**). Overall, pharmacological and genetic data indicate that c-Met and AXL are the causes of *UCA1*-mediated carboplatin resistance.

UCA1 functions as a ceRNA for miR-206 to facilitate AXL and c-Met expression in RB cells

Previous studies have revealed that *UCA1* utilises ceRNAs for specific miRNAs, resulting in the release of corresponding miRNA-targeted transcripts. To confirm this hypothesis, Y79 cells were transfected first to effectively block miRNA biogenesis by Dicer-specific siRNA. Interestingly, the increase in c-Met and AXL induced by *UCA1* was cancelled with the knockdown of Dicer (**Figure 4A**). To demonstrate the principal effect of miRNA on the effect, RIP analysis was implemented on Ago2, which is the core component of the silencing complex induced by RNA [22]. *UCA1* overexpression in Y79 cells led to upregulated Ago2 enrichment in *UCA1* but markedly downregulated enrichment of c-Met and AXL transcripts (**Figure 4B**). Simultaneously, the knockdown of *UCA1* in YCR3rd cells caused a significant upregulation in Ago2 recruitment of c-Met and AXL transcripts in comparison with control cells (**Figure 4C**). These results indicate that *UCA1* can com-

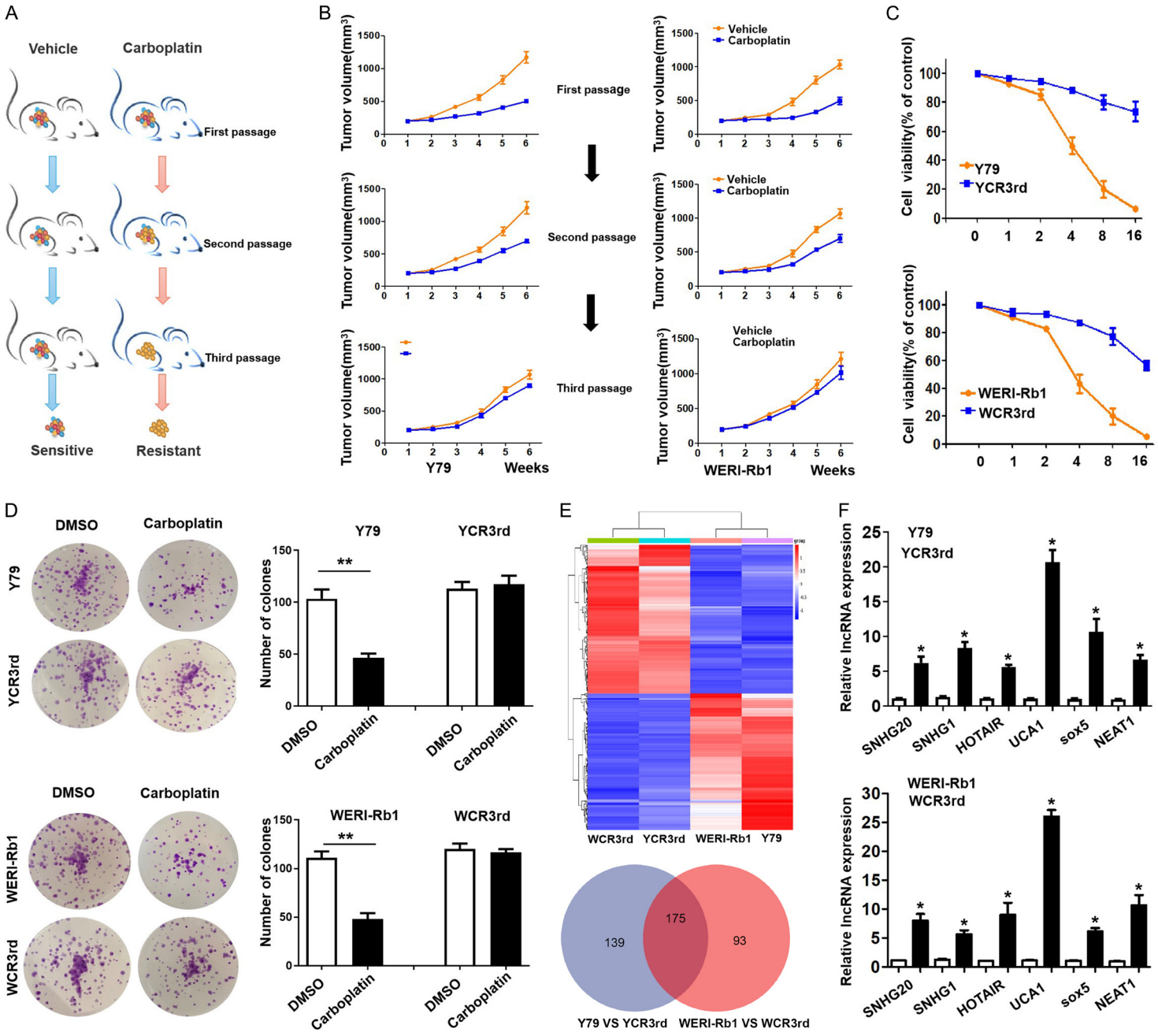
A
Vehicle
Carboplatin
First passage
Second passage
Third passage
Sensitive
Resistant
B
Tumor volume(mm3)
First passage
Second passage
Third passage
Vehicle
Carboplatin
Y79
Weeks
WERI-Rb1
Weeks
C
Cell viability(% of control)
Y79
YCR3rd
WERI-Rb1
WCR3rd
D
DMSO
Carboplatin
Y79
YCR3rd
WERI-Rb1
WCR3rd
Number of colones
E
WCR3rd
YCR3rd
WERI-Rb1
Y79
139
175
93
Y79 VS YCR3rd
WERI-Rb1 VS WCR3rd
F
Relative lncRNA expression
SNHG20
SNHG1
HOTAIR
UCA1
sox5
NEAT1

Figure 1. UCA1 is highly expressed in carboplatin-Resistant RB Cells. A. A schematic model of carboplatin resistant Rb cell process was obtained. B. Y79 or WERI-RB-1 xenografted nude mice were treated with carrier or carboplatin (n = 6). Tumor volume was expressed as mean ± SD. C. CCK8 of carboplatin resistant cells and parental cells was measured after treatment with carboplatin at the indicated concentration. D. Colony formation test of carboplatin resistant cells and parent cells after treatment in 12 well dishes for 3 weeks. E. Heat map displays thr microarray data of parental and CR cells. F. Differential lncrna (fold change > 5) was measured through qRT-PCR, *P < 0.05.

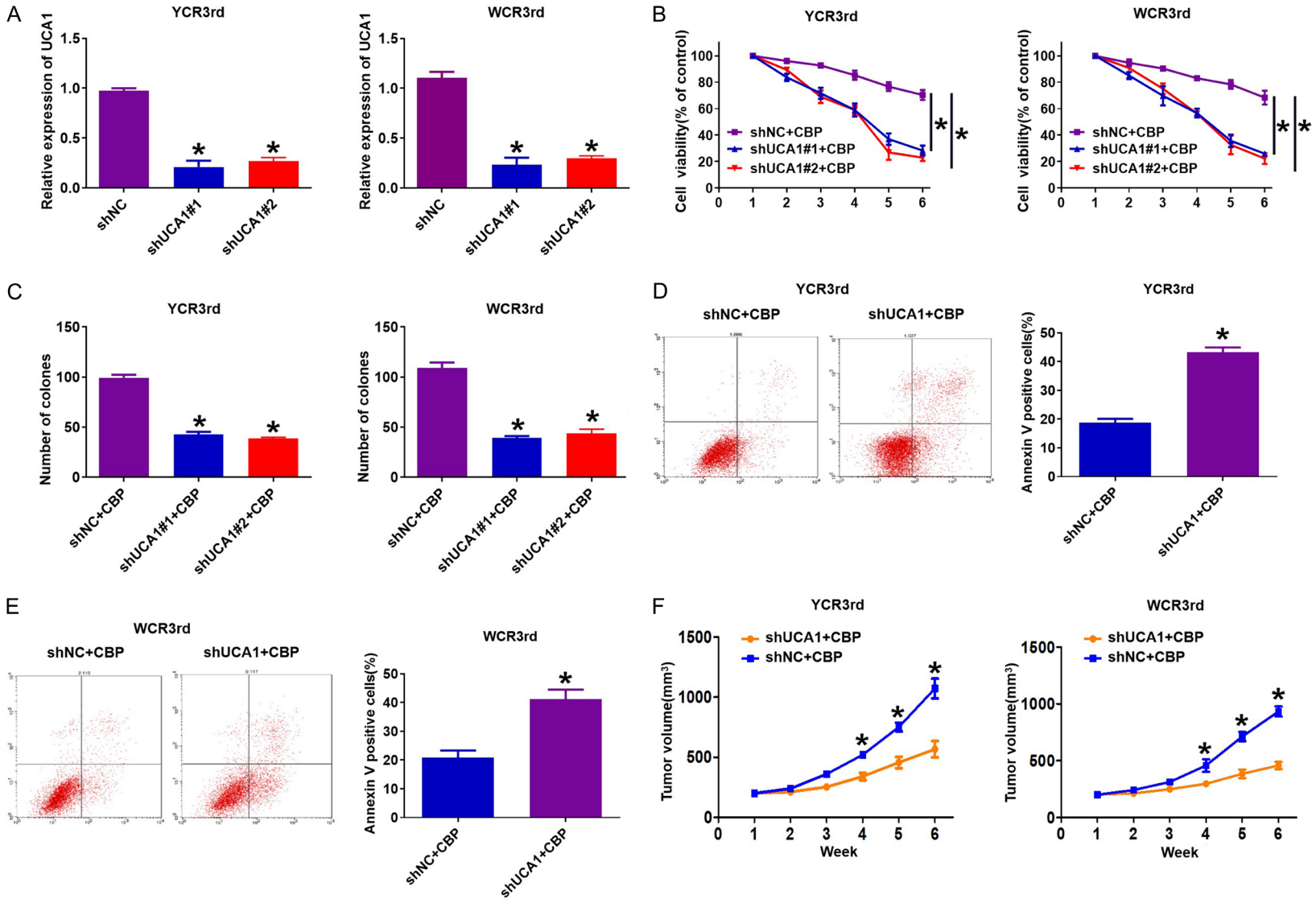

Figure 2. UCA1 is required for carboplatin Resistance of RB. A. qRT-PCR was applied for detecting the UCA1 silencing efficiency in CR cells. B. CCK8 detection of CR and UCA1-knockdown cells treated with carboplatin at specific concentrations (n = 3). *P < 0.05. C. Colony formation tests of UCA1 knockdown and control carboplatin resistant cells treated with carboplatin in 12-well petri dishes for 3 weeks. D, E. Apoptosis was detected by flow cytometry. F. Subcutaneous xenotransplantation of UCA1 knockdown and control carboplatin resistant cells was performed in nude mice treated with carboplatin (n = 6). *P < 0.05.

pete with c-Met and AXL transcripts for inhibitory complexes induced by miRNAs based on Ago2.

Next, we investigated *UCA1* distribution in RB cells. The results suggested that in Y79 cells, *UCA1* was present in both the nucleus and cytoplasm; however, the proportion of *UCA1* in the nucleus was much lower than that in the cytoplasm (**Figure 4D**). Moreover, we searched for miRNAs containing *UCA1* complementary base pairs using Starbase v2.0. Bioinformatics analyses revealed that *UCA1* shared the miRNA response element (MRE) of miR-206 and the 3'UTR of c-Met and AXL (**Figure 4E**). In addition, a comparable copy number of *UCA1* and miR-206 was detected in each CR cell (**Figure 4F** and **4G**), which is significant for the cerNa-mirNA interactions. Transfection with miR-206 mimics markedly suppressed the luciferase activity of psiCHECK-UCA1/WT, and psiCHECK-UCA1/MUT did not respond to miR-206 mimics (**Figure 4H** and **4I**). These results suggest that *UCA1* contains functional miR-206 binding sites.

In addition, the inhibition of miR-206 with miR-206 inhibitors was sufficient to restore carboplatin resistance after *UCA1* knockdown (**Figure 5A** and **5B**). In contrast, the use of the miR-206 simulant eliminated the carboplatin resistance mediated by *UCA1* (**Figure 5C** and **5D**). Next, we investigated whether *UCA1*-mediated miR-206 isolation was associated with the upregulation of c-Met and AXL. A pGL3 reporter involving mutant (MUT) or wild-type miR-206 MRE and c-Met or Axl 3'UTR was established (**Figure 5E**). After the knockdown of *UCA1*, the luciferase activity of c-Met and AXL reporter was downregulated, which was reduced by miR-206 suppression, whereas the MUT reporter luciferase activity remained unchanged (**Figure 5F**). Conversely, after transfection with pcDNA3.1-UCA1, the luciferase activity of c-Met and AXL wild-type reporters was upregulated in a dose-dependent manner, whereas the overexpression of miR-206 eliminated this effect (**Figure 5G**). These outcomes were further demonstrated at the protein and RNA levels of c-Met and AXL (**Figure 5H** and **5I**). In conclusion, these findings suggest that *UCA1*, as a molecular sponge of miR-206, facilitates c-Met and AXL expression.

Targeting UCA1 restores carboplatin response in RB

To assess the therapeutic potential of *UCA1* in CR RB *in vivo*, we used a modified LNA targeting *UCA1* in an *in situ* Y79CR-RLUC cell xenograft model. Bioluminescence imaging revealed that the therapeutic *UCA1* LNA can restore the sensitivity of Y79CR-RLUC xenografts to concurrent carboplatin therapy. After 28 days, the treatment was completed; however, tumour regeneration was not observed even after 42 days in the combined group (**Figure 6A-C**). This was related to the remarkably longer survival of the mice (**Figure 6D**). Furthermore, LNA-mediated *UCA1* knockdown and reduced AXL and C-Met levels were confirmed by qRT-PCR analysis (**Figure 6E**). Because c-Met and AXL are associated with carboplatin resistance mediated by *UCA1*, BMS777607 was studied *in vivo*. BMS777607 combined with carboplatin significantly inhibited the growth of CR xenografts although neither of them alone resulted in growth inhibition (**Figure 6F**). Taken together, these data indicate that AXL or *UCA1* together with C-Met may be employed as latent therapeutic targets for eliminating resistance to carboplatin therapy in patients with RB.

Discussion

Carboplatin is a common chemotherapeutic drug for RB; however, carboplatin resistance in patients with RB is still the main obstacle to the success of chemotherapy [23, 24]. Increasing evidence indicates that the abnormal expression of lncRNA is involved in the chemoresistance of cancer and provides new insights into tumour progression biology [25]. Recently, *UCA1* was found to be upregulated in different types of cancer and to play a key role in chemoresistance [26]. Here, we focused on

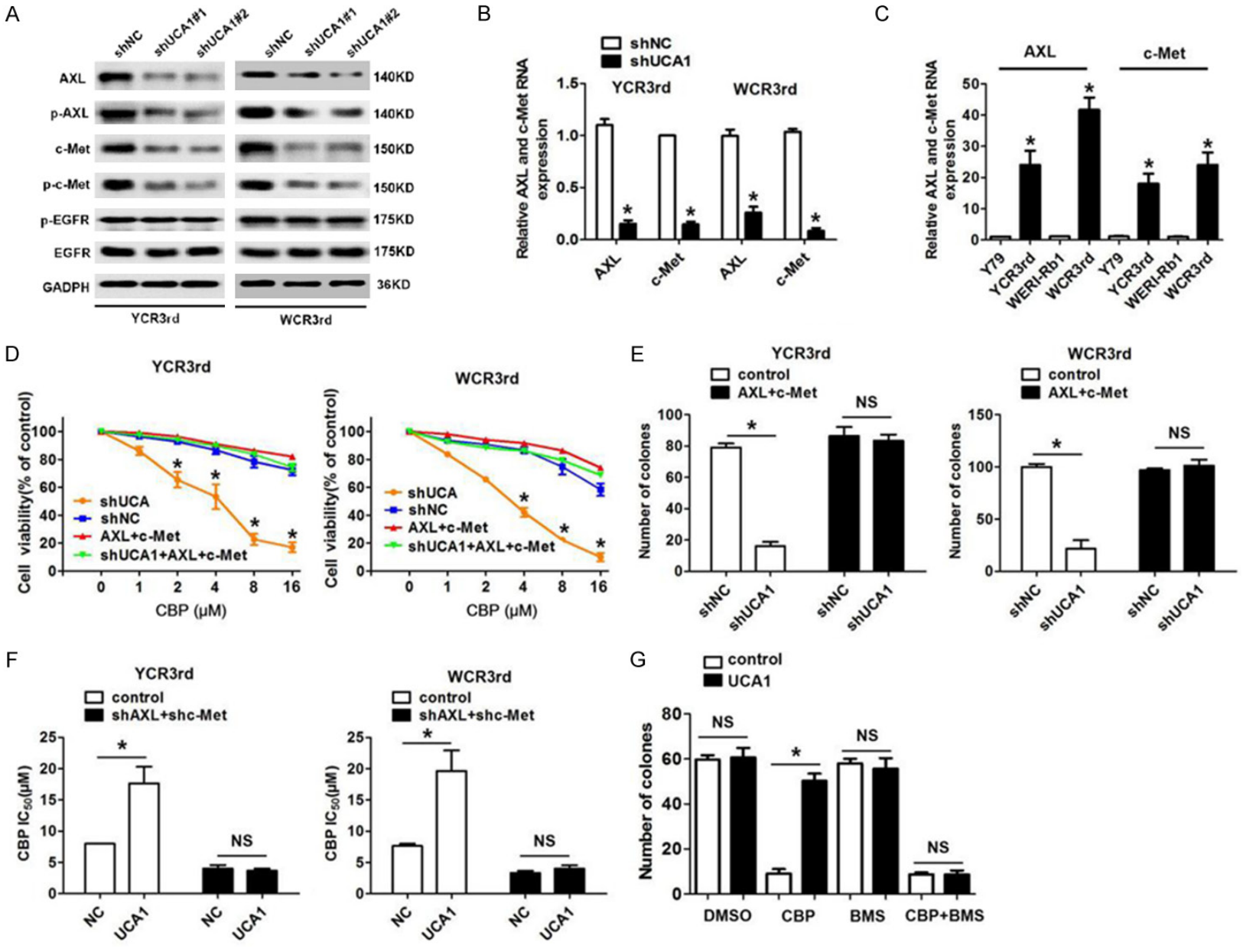
A
shNC
shUCA1#1
shUCA1#2
AXL
p-AXL
c-Met
p-c-Met
p-EGFR
EGFR
GADPH
140KD
140KD
150KD
150KD
175KD
175KD
36KD
YCR3rd
WCR3rd
B
shNC
shUCA1
YCR3rd
WCR3rd
Relative AXL and c-Met RNA expression
AXL
c-Met
C
AXL
c-Met
Relative AXL and c-Met RNA expression
Y79
YCR3rd
WERI-Rb1
WCR3rd
D
YCR3rd
WCR3rd
Cell viability(% of control)
shUCA
shNC
AXL+c-Met
shUCA1+AXL+c-Met
CBP (μM)
E
YCR3rd
WCR3rd
control
AXL+c-Met
Number of colones
NS
shNC
shUCA1
F
YCR3rd
WCR3rd
control
shAXL+shc-Met
CBP IC50(μM)
NS
NC
UCA1
G
control
UCA1
Number of colones
NS
DMSO
CBP
BMS
CBP+BMS

Figure 3. AXL and c-Met are key for UCA1-Mediated carboplatin resistance. A. The c-Met, AXL, and EGFR expressions together with their phosphorylated forms were detected by Western blot. B. qRT-PCR assay of c-Met and AXL in UCA1 gene down regulated and control carboplatin resistant RB cells (n = 3). *p is less than 0.05. C. qRT-PCR assay of c-Met and AXL in control and carboplatin resistant RB cells. D. CCK8 assay of YCR3rd or WCR3rd cells transfected with shUCA1 or p-c-Met and p-AXL at the specified concentration of carboplatin (n = 3). E. UCA1- knockdown and control YCR3rd or WCR3rd cells were transfected in 12 well dishes for 3 weeks (n = 3). F. The overexpression of UCA1 transfected with indicator plasmid and the IC50 of carboplatin in control RB cells were measured by CCK8 method (n = 3). *P < 0.05. G. Over expressing UCA1 and control RB cells were treated with carboplatin or BMS777607 (1 mm) and cultured in 12 well dishes for 3 weeks (n = 3). *P < 0.05.

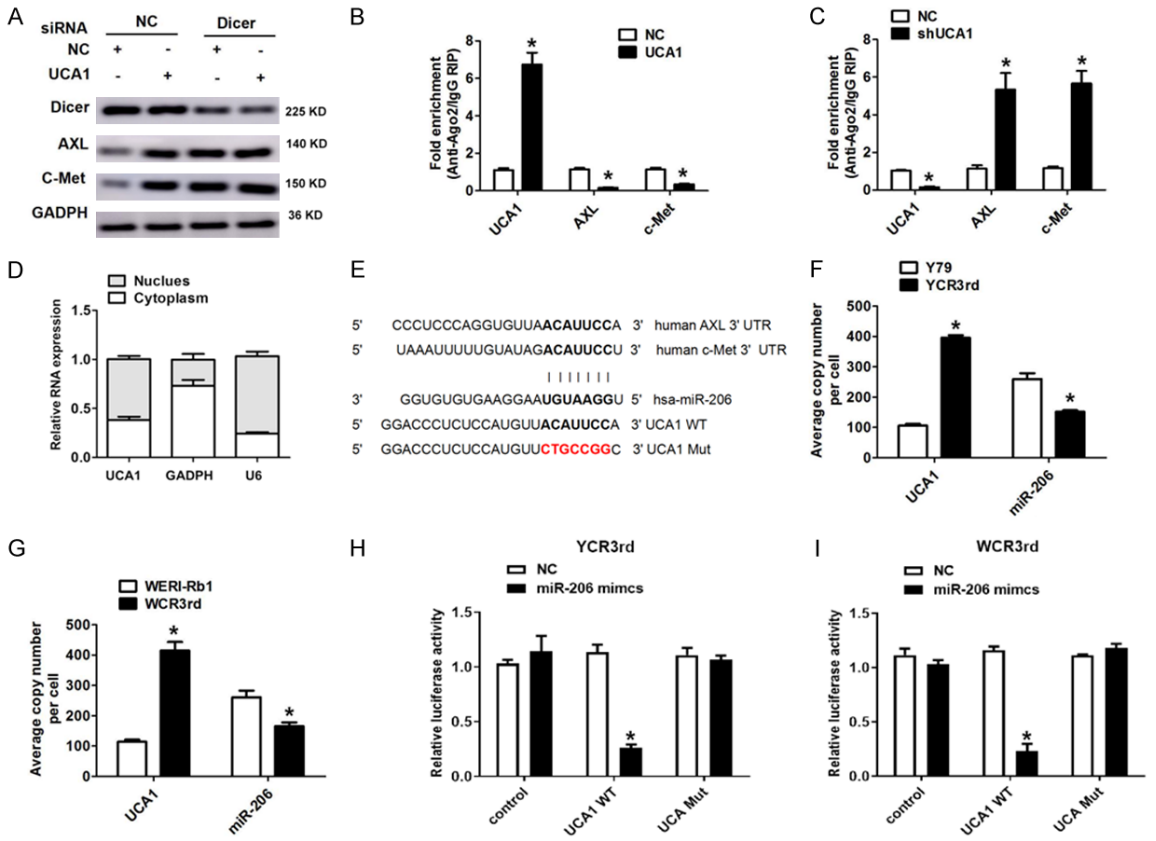

Figure 4. UCA1 Functions as a ceRNA for miR-206. A. Western blot detection of specific proteins in the Y79 cells transfected by Dicer specific UCA1 and siRNAs. B. RIP detection of Ago2 enrichment on the transcripts of c-Met, AXL, and UCA1 relative to IgG in the Y79 cells transfected via UCA1 and Control. C. RIP analysis of the Ago2 enrichment on the transcripts of c-Met, AXL, UCA1 relative to IgG in the YCR3rd cells transfected through shUCA1 and Control. D. qRT-PCR assay of the levels of UCA1 cytoplasmic and nuclear expression in the Y79 cells. U6 and GAPDH was employed as the nucleus marker and cytosol marker. E. Putative miR-206 MREs in the 3'UTR of c-Met, AXL and UCA1. The seed sequences are shown in bold and mutant sequences shown in red. F and G. qPCR analysis of the copy numbers of UCA1 and miR-206 in carboplatin-resistant and parental RB cells (n = 3). H, I. Luciferase activity in YCR3rd or WCR3rd cells co-transfected via luciferase reporters and miR-206 mimics involving nothing, UCA1 mut or UCA1 wt transcripts. **P < 0.01.

the mechanism of carboplatin resistance in RB cells mediated by *UCA1*. The results of our study indicated that *UCA1* was significantly upregulated in CR RB cells. In addition, *UCA1* gene knockdown reduced carboplatin resistance in CR RB cells. In particular, our results also revealed that the activation of alternative RTKs was associated with *UCA1*-mediated carboplatin resistance. Consistent with our results, *UCA1* is upregulated in gemcitabine- or cisplatin-resistant bladder cancer cells, and forced *UCA1* expression induces chemical resistance by facilitating cell proliferation and suppressing cell apoptosis.

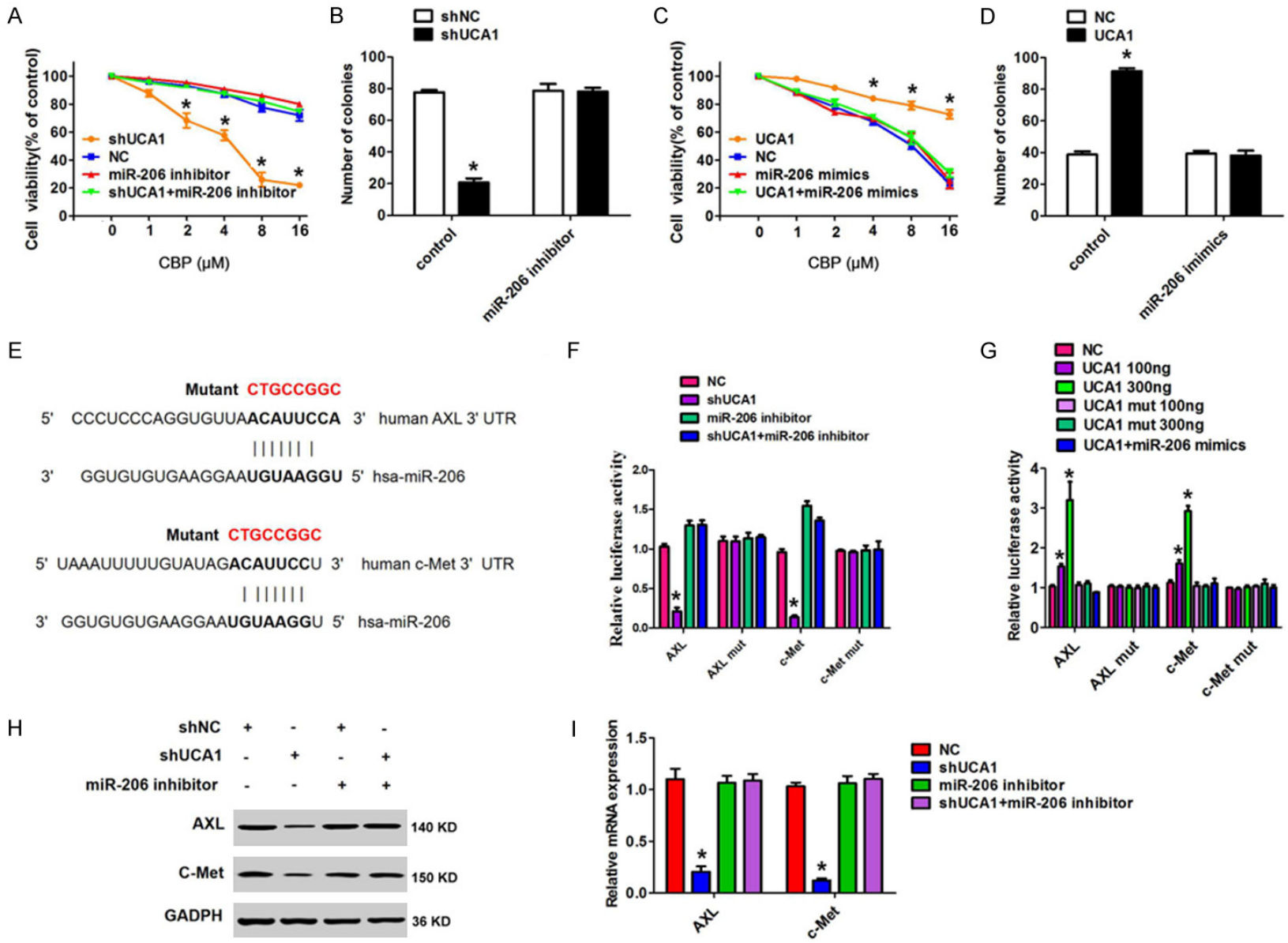
A
Cell viability(% of control)
shUCA1
NC
miR-206 inhibitor
shUCA1+miR-206 inhibitor
CBP (μM)
B
shNC
shUCA1
Number of colonies
control
miR-206 inhibitor
C
Cell viability(% of control)
UCA1
NC
miR-206 mimics
UCA1+miR-206 mimics
CBP (μM)
D
NC
UCA1
Number of colonies
control
miR-206 imimics
E
Mutant CTGCCGGC
5' CCCUCCCAGGUGUUAACAUUCCA 3' human AXL 3' UTR
3' GGUGUGUGAAGGAAUGUAAGGU 5' hsa-miR-206
Mutant CTGCCGGC
5' UAAAUUUUUGUAUAGACAUUCCU 3' human c-Met 3' UTR
3' GGUGUGUGAAGGAAUGUAAGGU 5' hsa-miR-206
F
NC
shUCA1
miR-206 inhibitor
shUCA1+miR-206 inhibitor
Relative luciferase activity
AXL
AXL mut
c-Met
c-Met mut
G
NC
UCA1 100ng
UCA1 300ng
UCA1 mut 100ng
UCA1 mut 300ng
UCA1+miR-206 mimics
Relative luciferase activity
AXL
AXL mut
c-Met
c-Met mut
H
shNC
shUCA1
miR-206 inhibitor
AXL
140 KD
C-Met
150 KD
GADPH
36 KD
I
Relative mRNA expression
NC
shUCA1
miR-206 inhibitor
shUCA1+miR-206 inhibitor
AXL
c-Met

Figure 5. UCA1 functions as a ceRNA for miR-206 to facilitate expression of AXL and c-Met. A. CCK8 detection of RB transfected through miR-206 and shUCA1 suppression after treating with carboplatin at specific concentrations (n = 3). *P is less than 0.05. B. Colony generation detection of control and UCA1-knockdown cells transfected via miR-206 suppression with the treatment of carboplatin in 12-well dish for three weeks (n = 3). *P is less than 0.05. C. CCK8 analysis of RB cells transfected by miR-206 and UCA1 mimics upon treatment of carboplatin at specific concentrations (n = 3). *P < 0.05. D. Colony generation analysis of control and UCA1-overexpressing RB cells transfected by miR-206 mimics after treated with carboplatin in 12-well dish for three weeks (n = 3). *P < 0.05. E. Putative miR-206 MREs in the 3'UTR of c-Met and AXL. The seed sequences are shown in bold and mutant sequences shown in red. F, G. The luciferase activity of pGL3 reporters which involved c-MET 3'UTR and mut or wild-type (miR-206 MREs) AXL with specific treatment in the RB cells (n = 3). *P < 0.05. H. Western blot detection of c-Met and AXL in RB cells transfected by shUCA1 or control together with miR-206 suppression. I. qRT-PCR assay of c-MET and AXL in RB cells transfected via shUCA1 or control together with miR-206 suppression. *P < 0.05.

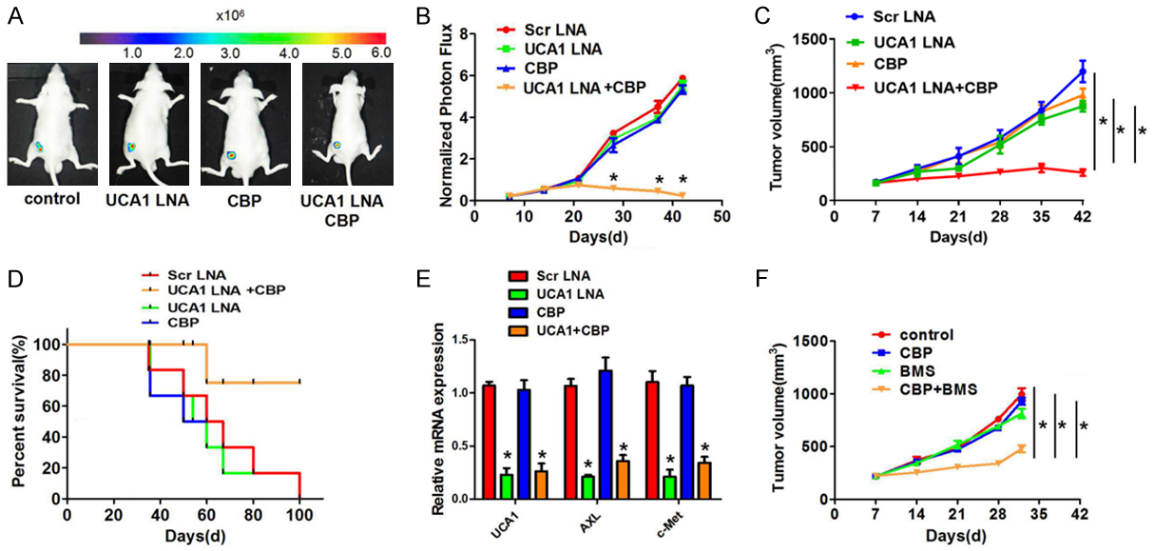

Figure 6. UCA1-knockdown Restores Carboplatin Response in vivo. (A-C) Orthotopic xenotransplantation of YCR3rd cells from nude mice was performed by intravenous injection of Scramble or UCA1 LNA twice weekly and oral administration of solvent or carboplatin daily (n = 6). Representative bioluminescence image (A), Tumor volume (B), quantization of bioluminescence imaging signal intensity (C), *P < 0.05. (D) Show the survival rate of mice in indicator group. (E) qRT-PCR analysis of specified transcripts from YCR3rd-luC xenograft after specified treatment (n = 6). *P < 0.05. (F) YCR3rd cells were subcutaneously transplanted into nude mice, and carrier or carboplatin and BMS777607 were taken orally daily. Tumor volume (n = 6). *P < 0.05.

lncRNAs interact with miRNAs to play the role of ceRNAs and regulate the inhibition of miRNA targets [27-29]. There is increasing evidence that *UCA1* acts as an oncogenic lncRNA by interacting with and inhibiting tumour-suppressor miRNAs such as miR-135a [30], miR-203 [31] and miR-204-5p [32]. Based on bioinformatics and luciferase reports, we identified the binding site of tumour-inhibiting miR-206 in *UCA1* and the 3'UTR of c-Met and AXL. Importantly, we observed that the introduction of miR-206 simulators eliminated *UCA1*-mediated carboplatin resistance in RB cells. Our observations are consistent with a recently published report suggesting that *UCA1* promotes cisplatin resistance via the miR-184-SF1 pathway in oral squamous cell carcinoma. Similar to miR-184, it has also been reported that miR-184 is a negative regulator of tumour suppressor genes and drug resistance. Therefore, *UCA1* may act as an oncogene by adsorbing drug-resistant miRNAs.

Elucidating the molecular basis of carboplatin resistance is helpful in developing reasonably designed combination therapies that block compensatory signalling pathways [33-35]. Our results show that in orthotopic xenotransplantation and PDX models, the inhibition of *UCA1* by LNA makes CR RB cells sensitive to carboplatin, which indicates that lncRNA-targeted treatment can be applied as an efficient method for treating CR RB. We also provide evidence of the use of c-Met and AXL inhibitors (UCA1

downstream effectors) to restore *UCA1*-mediated carboplatin resistance. According to our study, CR RB treatment with locking nucleic acid targeting the suppression of c-Met and AXL can restore the carboplatin reaction. These outcomes reinforce the concept that carboplatin resistance can be overcome by combination therapy targeting specific drug resistance mechanisms.

In conclusion, our results provide insights into the mechanism, emphasising that *UCA1* may upregulate the expression of its target genes, c-Met and AXL, in RB by utilising as the ceRNA of miR-206 to facilitate carboplatin resistance. In addition, in drug-resistant retinal cell lines, *in vivo* experiments showed that only UCA1 LNA had no effect on carboplatin resistance of drug-resistant cells, suggesting that other mechanisms of UCA1 affecting carboplatin resistance of drug-resistant cell lines need to be further explored. This study demonstrates the effect of *UCA1* in RB chemotherapy resistance, revealing that *UCA1* can be applied as a new marker of carboplatin adverse reactions and an underlying therapeutic target of RB chemotherapy.

Acknowledgements

This study was supported by a grant from the National Natural Science Foundation of China (grant Nos. 81960491 and 81460088). We would like to thank Editage (www.editage.cn) for English language editing.

Disclosure of conflict of interest

None.

Address correspondence to: Zhipeng You and Qifang Jin, Department of Ophthalmology, The Second Affiliated Hospital of Nanchang University, Nanchang 330006, Jiangxi, China. E-mail: zpdoctor78@126.com (ZPY); qifangefy6767@126.com (QFJ)

References

[1] Fabian ID, Onadim Z, Karaa E, Duncan C, Chowdhury T, Scheimberg I, Ohnuma SI, Reddy MA and Sagoo MS. The management of retinoblastoma. Oncogene 2018; 37: 1551-1560.

[2] Hadjistilianou T, Giglioni S, Micheli L, Vannoni D, Brogi E, Cevenini G, Cortelazzo A, De Francesco S, Menicacci F and Leoncini R. Analysis of aqueous humour proteins in patients with retinoblastoma. Clin Exp Ophthalmol 2012; 40: e8-e15.

[3] Català-Mora J, Parareda-Salles A, Vicuña-Muñoz CG, Medina-Zurinaga M and Prat-Bartomeu J. Uveitis masquerade syndrome as a presenting form of diffuse retinoblastoma. Arch Soc Esp Oftalmol 2009; 84: 477-480.

[4] Monroe EJ, Chick JFB, Stacey AW, Millard NE, Geyer JR, Ramoso LR, Ghodke BV and Hallam DK. Radiation dose reduction during intra-arterial chemotherapy for retinoblastoma: a retrospective analysis of 96 consecutive pediatric interventions using five distinct protocols. Pediatr Radiol 2021; 51: 649-657.

[5] Rajagopal T, Talluri S, Akshaya RL and Dunna NR. HOTAIR LncRNA: a novel oncogenic propellant in human cancer. Clin Chim Acta 2020; 503: 1-18.

[6] Peng WX, Koirala P and Mo YY. LncRNA-mediated regulation of cell signaling in cancer. Oncogene 2017; 36: 5661-5667.

[7] Kopp F and Mendell JT. Functional classification and experimental dissection of long noncoding RNAs. Cell 2018; 172: 393-407.

[8] Dai D, Wang H, Zhu L, Jin H and Wang X. N6-methyladenosine links RNA metabolism to cancer progression. Cell Death Dis 2018; 9: 124.

[9] Wang H, Huo X, Yang XR, He J, Cheng L, Wang N, Deng X, Jin H, Wang N, Wang C, Zhao F, Fang J, Yao M, Fan J and Qin W. STAT3-mediated upregulation of lncRNA HOXD-AS1 as a ceRNA facilitates liver cancer metastasis by regulating SOX4. Mol Cancer 2017; 16: 136.

[10] Li Y, Li L, Wang Z, Pan T, Sahni N, Jin X, Wang G, Li J, Zheng X, Zhang Y, Xu J, Yi S and Li X. LncMAP: pan-cancer atlas of long noncoding RNA-mediated transcriptional network perturbations. Nucleic Acids Res 2018; 46: 1113-1123.

[11] Zhang M, Wang N, Song P, Fu Y, Ren Y, Li Z and Wang J. LncRNA GATA3-AS1 facilitates tumour progression and immune escape in triple-negative breast cancer through destabilization of GATA3 but stabilization of PD-L1. Cell Prolif 2020; 53: e12855.

[12] Lingadahalli S, Jadhao S, Sung YY, Chen M, Hu L, Chen X and Cheung E. Novel lncRNA LINC00844 regulates prostate cancer cell migration and invasion through AR signaling. Mol Cancer Res 2018; 16: 1865-1878.

[13] Huang Z, Zhou JK, Peng Y, He W and Huang C. The role of long noncoding RNAs in hepatocellular carcinoma. Mol Cancer 2020; 19: 77.

[14] Xie W, Chu M, Song G, Zuo Z, Han Z, Chen C, Li Y and Wang ZW. Emerging roles of long noncoding RNAs in chemoresistance of pancreatic cancer. Semin Cancer Biol 2020; [Epub ahead of print].

[15] Nie W, Ge HJ, Yang XQ, Sun X, Huang H, Tao X, Chen WS and Li B. LncRNA-UCA1 exerts oncogenic functions in non-small cell lung cancer

by targeting miR-193a-3p. Cancer Lett 2016; 371: 99-106.
[16] Wu H and Zhou C. Long non-coding RNA UCA1 promotes lung cancer cell proliferation and migration via microRNA-193a/HMGB1 axis. Biochem Biophys Res Commun 2018; 496: 738-745.
[17] Xian Z, Hu B, Wang T, Zeng J, Cai J, Zou Q and Zhu P. lncRNA UCA1 contributes to 5-fluorouracil resistance of colorectal cancer cells through miR-23b-3p/ZNF281 axis. Onco Targets Ther 2020; 13: 7571-7583.
[18] Gao Q, Fang X, Chen Y, Li Z and Wang M. Exosomal lncRNA UCA1 from cancer-associated fibroblasts enhances chemoresistance in vulvar squamous cell carcinoma cells. J Obstet Gynaecol Res 2021; 47: 73-87.
[19] Fang Z, Zhao J, Xie W, Sun Q, Wang H and Qiao B. LncRNA UCA1 promotes proliferation and cisplatin resistance of oral squamous cell carcinoma by sunppressing miR-184 expression. Cancer Med 2017; 6: 2897-2908.
[20] Mirshafiey A, Ghalamfarsa G, Asghari B and Azizi G. Receptor tyrosine kinase and tyrosine kinase inhibitors: new hope for success in multiple sclerosis therapy. Innov Clin Neurosci 2014; 11: 23-36.
[21] Schroeder GM, An Y, Cai ZW, Chen XT, Clark C, Cornelius LA, Dai J, Gullo-Brown J, Gupta A, Henley B, Hunt JT, Jeyaseelan R, Kamath A, Kim K, Lippy J, Lombardo LJ, Manne V, Oppenheimer S, Sack JS, Schmidt RJ, Shen G, Stefanski K, Tokarski JS, Trainor GL, Wautlet BS, Wei D, Williams DK, Zhang Y, Zhang Y, Fargnoli J and Borzilleri RM. Discovery of N-(4-(2-amino-3-chloropyridin-4-yloxy)-3-fluorophenyl)-4-ethoxy-1-(4-fluorophenyl)-2-oxo-1,2-dihydropyridine-3-carboxamide (BMS-777607), a selective and orally efficacious inhibitor of the Met kinase superfamily. J Med Chem 2009; 52: 1251-1254.
[22] Gregory RI, Chendrimada TP, Cooch N and Shiekhattar R. Human RISC couples microRNA biogenesis and posttranscriptional gene silencing. Cell 2005; 123: 631-640.
[23] Geng W, Ren J, Shi H, Qin F, Xu X, Xiao S, Jiao Y and Wang A. RPL41 sensitizes retinoblastoma cells to chemotherapeutic drugs via ATF4 degradation. J Cell Physiol 2021; 236: 2214-2225.
[24] Zhu X, Xue L, Yao Y, Wang K, Tan C, Zhuang M, Zhou F and Zhu L. The FoxM1-ABCC4 axis mediates carboplatin resistance in human retinoblastoma Y-79 cells. Acta Biochim Biophys Sin (Shanghai) 2018; 50: 914-920.
[25] Wang Y, Xin D and Zhou L. LncRNA LINC00-152 increases the aggressiveness of human retinoblastoma and enhances carboplatin and Adriamycin resistance by regulating MiR-613/yes-associated protein 1 (YAP1) axis. Med Sci Monit 2020; 26: e920886.
[26] Li C, Fan K, Qu Y, Zhai W, Huang A, Sun X and Xing S. Deregulation of UCA1 expression may be involved in the development of chemoresistance to cisplatin in the treatment of non-small-cell lung cancer via regulating the signaling pathway of microRNA-495/NRF2. J Cell Physiol 2020; 235: 3721-3730.
[27] Karreth FA and Pandolfi PP. ceRNA cross-talk in cancer: when ce-bling rivalries go awry. Cancer Discov 2013; 3: 1113-1121.
[28] Zhu J, Zhang X, Gao W, Hu H, Wang X and Hao D. lncRNA/circRNA-miRNA-mRNA ceRNA network in lumbar intervertebral disc degeneration. Mol Med Rep 2019; 20: 3160-3174.
[29] Li JH, Liu S, Zhou H, Qu LH and Yang JH. starBase v2.0: decoding miRNA-ceRNA, miRNA-ncRNA and protein-RNA interaction networks from large-scale CLIP-Seq data. Nucleic Acids Res 2014; 42: D92-97.
[30] Li ZG, Xiang WC, Shui SF, Han XW, Guo D and Yan L. 11 long noncoding RNA UCA1 functions as miR-135a sponge to promote the epithelial to mesenchymal transition in glioma. J Cell Biochem 2020; 121: 2447-2457.
[31] Liu HE, Shi HH and Luo XJ. Upregulated long noncoding RNA UCA1 enhances Warburg effect via miR-203/HK2 axis in esophagal cancer. J Oncol 2020; 2020: 8847687.
[32] Liang C, Yang Y, Guan J, Lv T, Qu S, Fu Q and Zhao H. LncRNA UCA1 sponges miR-204-5p to promote migration, invasion and epithelial-mesenchymal transition of glioma cells via up-regulation of ZEB1. Pathol Res Pract 2018; 214: 1474-1481.
[33] Beshiri ML, Tice CM, Tran C, Nguyen HM, Sowalsky AG, Agarwal S, Jansson KH, Yang Q, McGowen KM, Yin J, Alilin AN, Karzai FH, Dahut WL, Corey E and Kelly K. A PDX/organoid biobank of advanced prostate cancers captures genomic and phenotypic heterogeneity for disease modeling and therapeutic screening. Clin Cancer Res 2018; 24: 4332-4345.
[34] Moyano-Galceran L, Pietilä EA, Turunen SP, Corvigno S, Hjerpe E, Bulanova D, Joneborg U, Alkasalias T, Miki Y, Yashiro M, Chernenko A, Jukonen J, Singh M, Dahlstrand H, Carlson JW and Lehti K. Adaptive RSK-EphA2-GPRC5A signaling switch triggers chemotherapy resistance in ovarian cancer. EMBO Mol Med 2020; 12: e11177.
[35] Barghout SH, Zepeda N, Xu Z, Steed H, Lee CH and Fu Y. Elevated β-catenin activity contributes to carboplatin resistance in A2780cp ovarian cancer cells. Biochem Biophys Res Commun 2015; 468: 173-178.

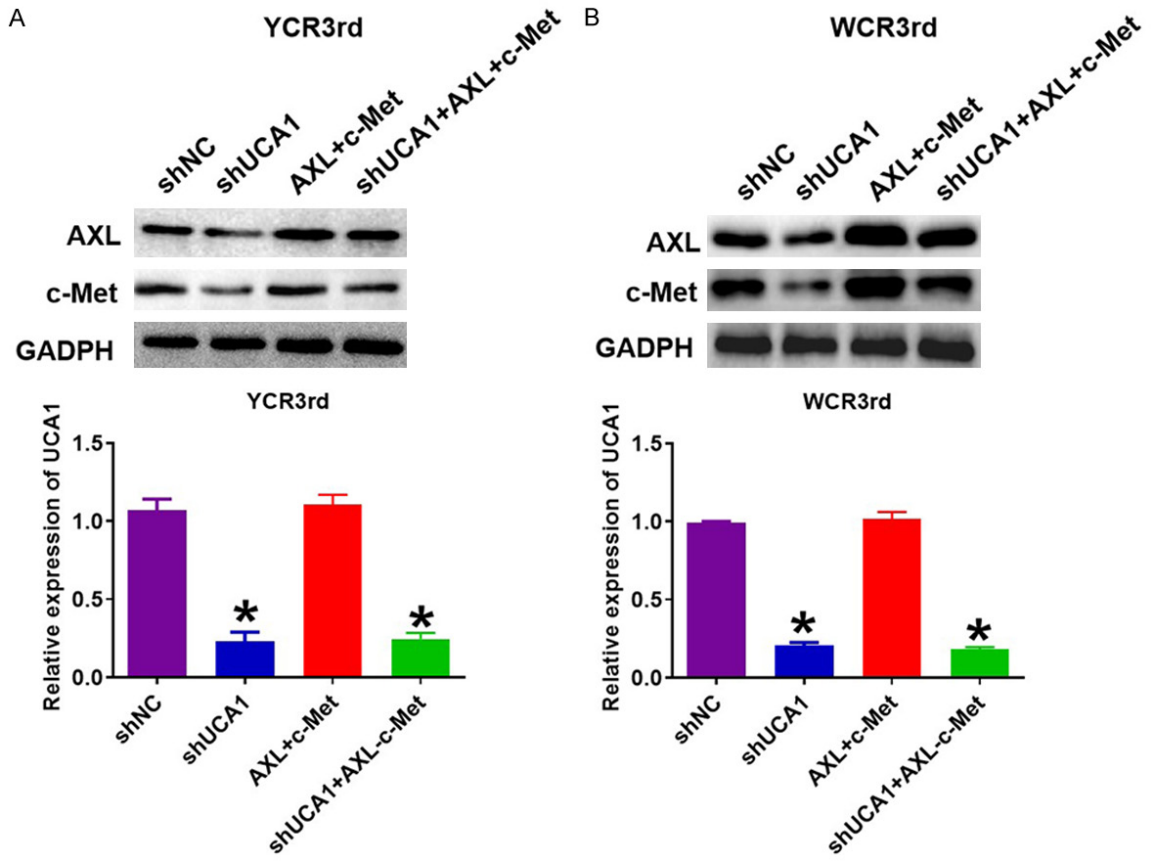

Supplementary Figure 1. A, B. The expression of c-Met and AXL protein were detected by Western blot,and the expression of UCA1 was detected by qRT-PCR.

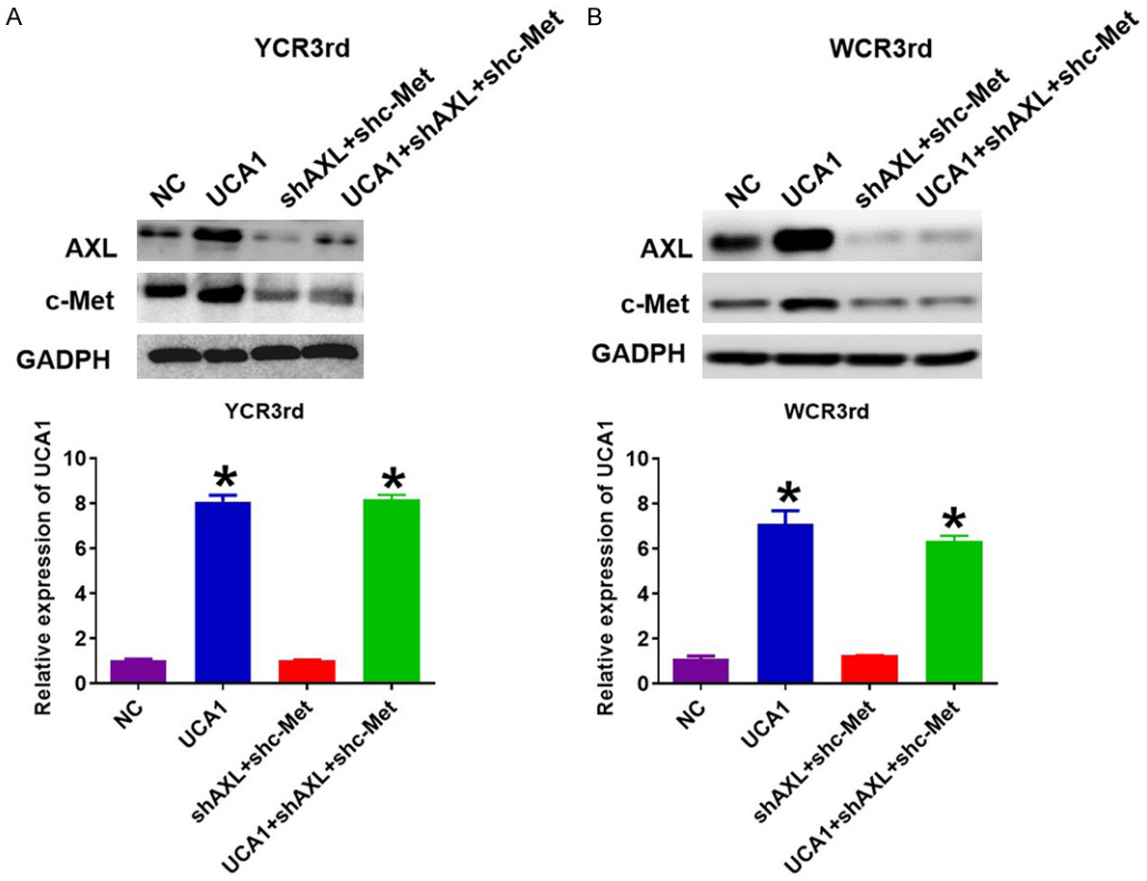

Supplementary Figure 2. A, B. The expression of c-Met and AXL protein were detected by Western blot,and the expression of UCA1 was detected by qRT-PCR.